

Revealing Photonic Properties with High Spatial Resolution: An EELS Study on Ceria Nanocubes

Yifan Wang^{1*}, Shize Yang² and Peter A. Crozier¹

¹ School for Engineering of Matter, Transport & Energy, Arizona State University, Tempe, AZ, United States.

² Eyring Materials Center, Arizona State University, Tempe, AZ, United States.

* Corresponding author: ywan1240@asu.edu

Nanoscale optics can be applied to various fields, e.g., sensor, energy harvesting, and communication [1]. A fundamental understanding of their properties is necessary to fulfill the potential of nano optics. However, the relatively low spatial resolution of traditional optical measurement methods, e.g., Raman spectroscopy and infrared spectroscopy, set an obstacle to study the photonic properties for nanoscale optical structures. By the Weizsäcker-Williams approximation [2–4], the electromagnetic field generated by high-speed charged particles (e.g., electron in transmission electron microscope (TEM)) can be approximated as virtual quanta, e.g. virtual photons. In other words, in TEM, electrons can be used as a light source with a higher spatial resolution. Another unmatched advantage of using TEM to detect optic properties is that it can simultaneously excite and detect energy loss process in a large range of energy, from infrared [5] to ultraviolet [6], through electron energy-loss spectroscopy (EELS) in a scanning TEM (STEM). In sub-micron-sized dielectric particles e.g., CeO₂ (ceria), light can be trapped in the form of photonic modes, providing opportunities for energy harvesting and information transfer. Here, we applied monochromated STEM EELS to study the photonic modes in a ceria cube.

A ceria nanocube with a size of around 200nm in a (100) orientation is shown in the high-angle annular dark-field (HAADF) image of **Figure 1a**. Monochromated EELS in the aloof configuration was performed on a Nion UltraSTEM 100, since relatively thick samples will cause a low signal to noise ratio in the spectra from transmission configuration due to high-angle elastic scattering beyond detection limit. To prevent transmission between part of the convergent beam and the nanoparticle, the impact parameter, *b*, which is the distance between probe and the particle surface, was set to 10 nm. **Figure 1b** shows spectra from two different points: the blue one, denoted as the edge setting, is near the top left edge of the cube, parallel to of the incident electron beam, and the red one, denoted as the face setting, is around the middle of the face of the cube. Four peaks between 2 eV and the bandgap edge (~3.40eV), denoted as peak I(~2.45eV), II(~2.65eV), III(~3.10eV), and IV(~3.25eV), are presenting in both spectra. In the face geometry, peaks II and III are the predominant peak, while peak IV is about half the intensity of peak III, and there is nearly no sign of peak I. For the edge setting, peaks I and IV are the strongest, while peak II has a low intensity, and peak III is covered by the tail of peak IV. **Figure 1c** presents the EELS intensity mapping of each peak across the cube. The dark square at the right top of each sub-figure is the nanocube. For peaks II and III, the high intensity region formed an arc-shape area, and the brightest area is at the middle part of the arc, close to the middle of the (100) surface. Meanwhile, peak I and peak IV give higher intensity near the edge of the cube.

Notice that the mappings of the peaks do not show perfect symmetric of a cube. To understand the slight asymmetry, we acquired spectra at several geometrically equivalent positions along the side of the cube (**Figure 2a**). **Figure 2b** and **2c** shows 2 sets of 3 spectra which give a matching result with the EELS mapping, and changes are observed in major peaks for both settings. For face setting (**Figure 2b**), *f*₂

shows an intensity decrease and peak broadening for both peak II and III comparing to f1 and f3, which are giving qualitatively identical results. For the edge settings (**Figure 2c**), e1 and e3 are equivalent to the edge setting result in figure 1b, whereas peak I and especially, peak IV damped when beam is placed at e2. According to the HAADF image, the surroundings of the cube do not guarantee a perfect symmetry as there is a huge cluster at the top right of the cube. Considering the travelling paths of the modes, modes generated from e1, e3, f1 and f3 are predominately bounded by vacuum interfaces, whereas for e2 and f2, one of the boundaries is associated with large aggregates. By Fresnel law [7], larger difference of refractive index before and after the boundary gives higher reflection probability and lower transmission probability. As suggested by Rayleigh-Gans approximation [8], ceria clusters will give a refractive index between the vacuum and ceria. Therefore, the modes travelling towards the large clusters have higher probability of transmitting out of the cube and decaying, giving lower intensity peaks. Further simulations using COMSOL Multiphysics [9] calculating EELS and electric field corresponding to the peaks were also performed, which would help us understand the more basic properties of the mode, e.g., the location where the modes' intensity peaks at, thus provide guidance for the application of the photonic modes [10].

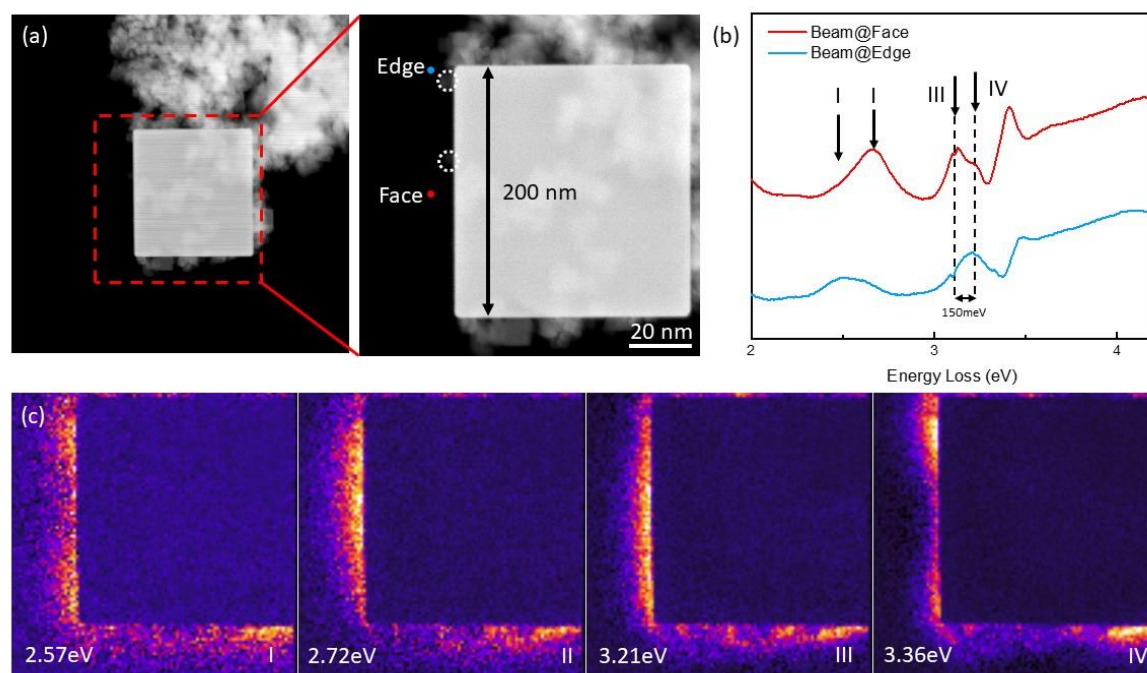


Figure 1. (a) STEM image of the cube and the position of the two points where the spectra were taken. The left face of the cube is nearly clean except two tiny cubes, denoted by dotted circle. Both points are 10 nm away from the cube. (b) The background-subtracted EELS spectra at two points. The energy of the four peaks is indicated by arrows. (c) The EELS mapping of the cube and surrounding region. The peak intensity is represented by the blackbody temperature of the color. Cold color (purple \rightarrow black) suggests a low intensity while warm color (orange \rightarrow white) indicates a high intensity. These four subfigures **do not** share the same intensity bar.

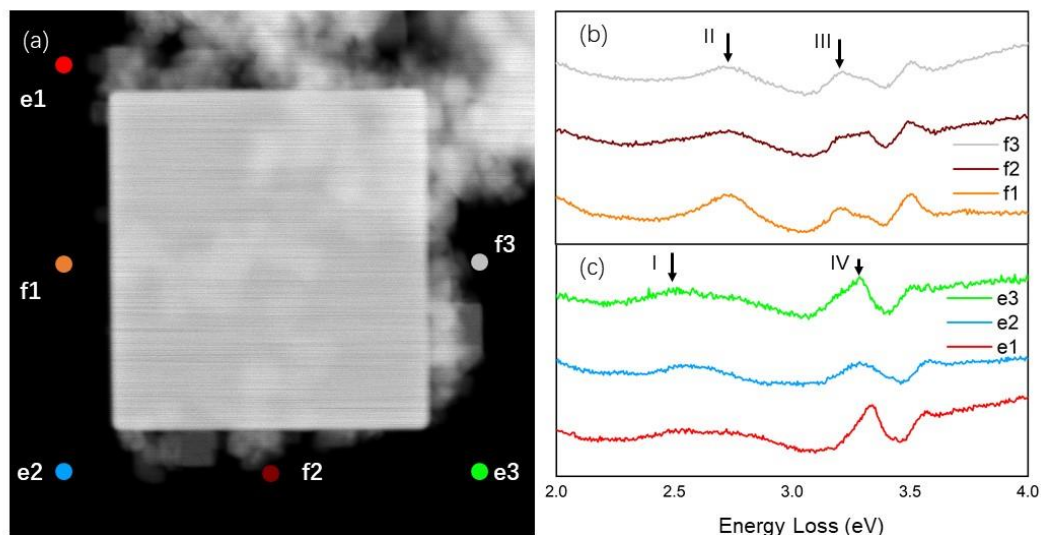


Figure 2. HAADF image and EELS point-scans extracted from EELS mapping at 2 set of geometry equivalent points. (a) The 6 points are showed in the HAADF image. The edge settings are denoted by e and face settings are denoted by f. (b-c) Two set of spectra shows the energy loss spectra corresponding to each point. (b) presents the face settings and (c) presents the edge settings. All the spectra are normalized to the zero-loss peak and plotted separately.

References:

- [1] A Fratlocchi et al., *Nat. Nanotechnol.* **10** (2015), p. 11.
- [2] E Fermi, *Zeitschrift Für Phys.* **29** (1924), p. 315.
- [3] CF v Weizsäcker, *Zeitschrift Für Phys.* **88** (1934), p. 612.
- [4] EJ. Williams, *K. Dan. Vidensk. Selsk. Mat. Fys. Medd.* **13** (1935).
- [5] OL Krivanek et al., *Nature* **514** (2014), p. 209.
- [6] RF Egerton in "Electron Energy-Loss Spectroscopy in the Electron Microscope" (Springer US, Boston, MA).
- [7] DJ Griffiths in "Introduction to Electrodynamics, Vol. 148" (Cambridge University Press).
- [8] CM Sorensen, *Aerosol Sci. Technol.* **35** (2001), p. 648.
- [9] A Konečná et al., *Phys. Rev. B* **98** (2018), p. 205409.
- [10] We gratefully acknowledge support of U.S. DOE (BES DE-SC0004954) and the use of ASU's John M. Cowley Center for High Resolution Electron Microscopy.